Accepted for publication in Canadian Journal of Fisheries and Aquatic Sciences, doi: 10.1139/cjfas-2016-0008: http://www.nrcresearchpress.com/doi/abs/10.1139/cjfas-2016-0008#.WDPddXrl-XC

Modeling the spatial distribution of larval fish abundance provides essential information for management

Meri Kallasvuo[1], Jarno Vanhatalo[2,3], Lari Veneranta[4]

[1]Natural Resources Institute Finland (Luke), Bioproduction of Renewable Resources, Viikinkaari 4, FI-00790 Helsinki, Finland, meri.kallasvuo@luke.fi

[2]Department of Mathematics and Statistics, University of Helsinki, Gustaf Hällströmin katu 2 B, P.O. Box 68, FI-00014 University of Helsinki, jarno.vanhatalo@helsinki.fi

[3]Department of Biosciences, University of Helsinki, Viikinkaari 1, P.O. Box 65, FI-00014 University of Helsinki, jarno.vanhatalo@helsinki.fi

[4]Natural Resources Institute Finland (Luke), Bioproduction of Renewable Resources, Korsholmanpuistikko 16, FI-65100 Vaasa, Finland, lari.veneranta@luke.fi

Corresponding author:

21 Meri Kallasvuo, Natural Resources Institute Finland (Luke), Bioproduction of Renewable
22 Resources, Viikinkaari 4, FI-00790 Helsinki, Finland, +358295327070,
23 meri.kallasvuo@luke.fi

Abstract

Productive fisheries are strongly linked to the ecological state of the essential habitats. In this study, we developed a methodology to assess the most important reproduction habitats of fish by using larval survey data and Bayesian species distribution models that predict the spatial distribution and abundance of fish larvae. Our case study with four commercially and ecologically important fish species in the coastal zone of the northern Baltic Sea demonstrated that the production of fish stocks can be concentrated to an extremely limited area compared to the entire suitable production area. The area suitable for larval production varied from 3.7% to 99.8% between species, but the smallest area responsible for 80% of the cumulative larval production was two to five times more limited, varying from 1.4% to 52.9% between species. Hence, instead of the traditional approach of modeling only habitat suitability for fish production, marine spatial planning and management should take into account the areal production potential. Moreover, the developed methodology enables linking of the total production potential across the whole distribution area to fisheries stock assessment and management.

Introduction

The water areas that fish use for reproduction or as nurseries are referred to as essential fish habitats (Cross et al. 1997; Benaka 1999), since fish usually have the most specific habitat demands during spawning and early life-stages. Hence, the size of the reproduction habitats forms a habitat bottleneck that limits fish production (Halpern et al. 2005; Sundblad et al. 2014). Essential fish habitats often exist in shallow coastal areas (Seitz et al. 2014), which are also heavily exploited and threatened by various anthropogenic pressures (Seitz et al. 2014; Sundblad and Bergström 2014). Therefore, there is a growing need to find concrete tools to manage coastal areas effectively and plan multiple uses and conservation to ensure that coastal resources and services are utilized sustainably.

During the last two decades, advances in marine habitat mapping and the development of geographic information system (GIS)-based tools for predicting species and habitat distributions (Guisan and Zimmermann 2000; Elith et al. 2006) have facilitated a detailed and explicit assessment of habitat availability. The main objectives in species distribution modeling are to predict the spatial and temporal occurrence or abundance pattern over a region of study and to identify the range of environmental covariates that best describe these patterns (Latimer et al. 2006; Austin 2007; Elith and Leathwick 2009). This information can also be used to predict species distributions under a changing environment.

Traditionally, species distribution models have focused on occurrence (Elith et al. 2006, Latimer et al. 2006). However, this approach fails to describe the abundance of a species, which may vary considerably between regions and habitats, and is essential information for management (Shelton et al. 2014; Thorson et al. 2015) and also for conservation purposes (Johnston et al. 2015). When abundance data, such as the number of

64 individuals observed at a survey site, are available, it is possible to model the density of a
65 species, i.e., the number of individuals within a given area (e.g. Vanhatalo et al., in press), or
66 in the case of fish, in a given volume of water (e.g. Juntunen et al. 2012; Shelton et al. 2014;
67 Thorson et al. 2015). The modeling outcome can then be presented as density maps that allow
68 a comprehensive numerical evaluation of the species distribution and essential habitats. For
69 example, those areas that are the most crucial for the total production of a fish stock can be
70 identified.
71 In this study, we used a GIS- and modeling-based, spatially explicit approach to
72 quantitatively assess the reproduction habitats of four commercially and ecologically
73 important fish species in the northern Baltic Sea by predicting the distribution and abundance
74 of their early life stages. We propose a novel approach to visualize and communicate the
75 results to managers and other end-users by classifying areas based on their predicted
76 contribution to the total production. As a result, we explicitly identify geographical areas that
77 host the most productive coastal habitats and show that very limited coastal areas, compared
78 to the total distribution area, can be crucial for fish production.
79
80 Materials and methods
81
82 Study species
83
84 The study considered four fish species that have both ecological and economic
85 significance in the northern Baltic Sea area. The Baltic herring (*Clupea harengus membras*)
86 is one of the most important pelagic species in the Baltic ecosystem and the most important
87 species for fisheries in the northern Baltic Sea (Söderkultalahti 2015). The perch (*Perca*

88 *fluviatilis*) and pikeperch (*Sander lucioperca*) are top predators and central species in the
89 coastal system. They are fished commercially and are also highly sought after by recreational
90 fishers (Söderkultalahti 2015). The smelt (*Osmerus eperlanus*) is a common species in
91 estuarine areas (Shpilev et al. 2005), but nowadays mainly fished in the Gulf of Bothnia, the
92 northernmost part of the Baltic Sea (Söderkultalahti 2015).
93 Three of the target species, the perch, pikeperch, and smelt, are of freshwater
94 origin, and the Baltic herring is of marine origin. All the target species spawn in the spring in
95 shallow (<10 m) coastal waters in the northern Baltic Sea (Aneer 1989; Lappalainen et al.
96 2003; Shpilev et al. 2005; Snickars et al. 2010). The two predatory species, perch and
97 pikeperch, have specific habitat requirements for their reproduction, selecting shallow,
98 vegetated, and sheltered bays that warm up early in the spring (Snickars et al. 2010;
99 Veneranta et al. 2011). The smelt is perhaps even more selective and exclusively spawns in
100 low salinity estuaries and river mouths (Urho et al. 1990; Shpilev et al. 2005). The perch,
101 pikeperch, and smelt usually spawn in one reproductive cohort. The timing mostly depends
102 on the development of spring temperatures (Lappalainen et al. 2003; Shpilev et al. 2005;
103 Snickars et al. 2010; Veneranta et al. 2011). The Baltic herring is the most flexible of the
104 studied species in its reproductive requirements, and spawns in several reproductive cohorts
105 on both vegetation and hard bottoms in relatively low salinity coastal waters over the entire
106 northern Baltic Sea (Aneer 1989; Parmanne et al. 1994). Despite some dissimilarity in their
107 life history, the larvae of all four species use coastal habitats during their entire first summer
108 (Sjöblom and Parmanne 1978; Urho and Hildén 1990; Sundblad et al. 2014).
109 Here, our main interest was in the early-stage larvae, which are found in the
110 open water within the archipelago zone, usually still relatively close to the spawning sites, at
111 approximately the same time of a year. It is not well known whether the larvae are only

present in the surface water layer or more uniformly also in the deeper water layers. However, in the spring, the water temperature is always highest near the surface, which makes it the most favorable location for the larvae. Therefore, here we sampled fish larvae only in the surface water layer.

Study area and data collection

The study area was located in the northern Baltic Sea, which is one of the largest brackish semi-enclosed seas in the world. The coastal areas of the northern Baltic Sea typically consist of extensive, shallow and topographically complex archipelagos, where the coastline is indented and long, the sea is covered with ice in the winter months, and tides and strong currents are absent (Voipio 1981). The study area covered the whole Finnish coastal region (N 59.8–65.8, E 19.1–27.8) of 30 100 km^2 in the northern Baltic Sea (Fig. 1). Environmental gradients are typically strong in the area, both north–south and west–east along the coastline, and also from inshore to offshore (Kallasvuo 2010). For example, surface salinity ranges from below 1 to almost 7 ppt and the spring temperature varies strongly between inner bays and open water areas.

To collect data on the distribution of the larvae of the four target species, an extensive field survey of the surface water layer was conducted in 2007–2014 with paired Gulf ichthyoplankton samplers, which have been used to quantitatively monitor the abundance and spatial occurrence of, for example, Baltic herring larvae (Sjöblom and Parmanne 1978; Parmanne and Sjöblom 1988; Urho and Hildén 1990) and pikeperch larvae (Veneranta et al. 2011). The Gulf samplers, with a mouth opening of 0.028 m^2, were attached bilaterally to the bow of the boat. The sampling was systematically conducted during the day

(8 am to 8 pm) over transects of 400 m (in 2007–2008) or 500 m (in 2009–2014) at a speed of 2.2 kn and only in good weather conditions (wind speed < 8 m/s, wave height < 30 cm). The paired samplers had fixed depths of 0.5 m and 1.0 m, and the catch and effort were pooled to form one sample observation with a total effort (volume) of 22.68 m^3 and 28.35 m^3 per shorter and longer transect, respectively. In 2014, at 18 very shallow, flad-type sampling sites, Gulf sampling with a boat was not possible to conduct, and a similar net as in the Gulf samplers was consequently used as a tow net. The tow net had a mouth opening of 0.166 m^2 and it was hauled over five 30-m-long transects per flad. The catch and effort were pooled, and the total sampling effort of one sample was 24.93 m^3. These observations are a proxy measure of larval abundance in units of count per effort, where the effort is the volume of sampled water.

All samples were fixed in the field with 4% formaldehyde solution, and species identification, counting, and measurement took place later in the laboratory. Since the aim was to describe the distribution of the most sensitive reproduction habitats, not the larger nursery areas, only early-stage larvae were included in the analysis. Our classification followed that of Urho (1996; 2002), with a larval size range of 4–23 mm for perch, 5–15 mm for pikeperch, and 4–36 mm for smelt. For Baltic herring, there is a known landward movement and concentration of larger larvae in very shallow inner bay areas (Urho and Hildén 1990), and we therefore used a more restrictive size range of 4–9 mm for Baltic herring larvae. In 2007 in the Archipelago Sea, length measurements were not available for Baltic herring larvae and the data from that year were not consequently used for the Baltic herring model.

The larval fish survey comprised a total of 1788 sampling occasions at 655 distinct sampling sites in 5 sea areas (Fig. 1). Sampling sites were dispersed over the entire

160 archipelago gradient, from the inner to the outer archipelago. In order to obtain survey results
161 that were as representative as possible, the sampling was stratified according to bottom depth
162 and exposure. Since different species hatch at different times, sampling was conducted two to
163 four times per year at intervals of about 10–14 days at each site during a period from mid-
164 May to early July. In order to remove sampling occasions that were sampled before or after
165 the larvae were present, we retained for each species only the sampling occasion with the
166 largest larval abundance per sampling site and per year, which resulted in 655 observations of
167 larval abundance per varying sampling effort. Each observation location was defined with
168 coordinates corresponding to the start location of the sampling transect.
169
170 Spatial environmental data
171
172 The larval fish survey data were linked to 15 environmental predictor covariates
173 falling into seven groups of covariates: depth, average depth, distance to deep water,
174 influence of rivers, shoreline density, exposure, and cumulative spring temperature
175 (summarized in detail in Table 1). The covariate depth corresponded to the actual depth at a
176 point measured from the depth model at maximum resolution, while the covariate average
177 depth described the water depth gradient on a large spatial scale. The covariate distance to
178 deep water indicated the location in the archipelago zone, e.g. sheltered inner bays were
179 emphasized. The covariate influence of rivers described the influence of freshwater runoff
180 from the river mouths. The covariate shoreline density, i.e. length of the shoreline in meters
181 in a grid cell, described the effect of wind exposure and water exchange, while the covariate
182 exposure described the degree of wave exposure. The covariate cumulative spring

183 temperature, i.e. the sum of daily sea surface temperatures from ice break up to July 15th,
184 described how rapidly the water area warmed up in the spring after ice break-up.
185 The covariate GIS rasters were mainly constructed during this study by the
186 authors, exceptions being depth, obtained from the Finnish Environment Institute (E.
187 Virtanen, Finnish Environment Institute, Helsinki, personal communication, 2015), and
188 exposure, which was obtained from AquaBiota Water Research (Isæus 2004). The influence
189 of rivers and shoreline density were calculated based on basic maps (scale 1:5000, National
190 Land Survey of Finland). The cumulative spring temperature was constructed by modeling
191 the cumulative temperatures from survey loggers located in the study region and predicting
192 the cumulative spring temperature for the entire study area (L. Veneranta, Natural Resources
193 Institute Finland, Vaasa, personal communication, 2015). In order to enable spatial
194 prediction, all covariates were in GIS raster format with the same extent and spatial
195 resolution of 50 m and covered the whole geographical extent of the study area (see Fig. 1).
196 The total number of grid cells across the study area was 12 040 218. Covariate values were
197 extracted for each observation from the grid cell in which that observation's starting point
198 was located. Even though each transect passed through 7-12 grid cells, we did not expect this
199 spatial misalignment to introduce large bias, since the environmental covariates were
200 approximately constant along all transects at a sampling site. Most of the environmental
201 variables were practically uncorrelated (the pairwise correlation in the data was less than 0.3),
202 but there was greater correlation between the depth, average depth, and distance to deep
203 water covariates (pairwise correlations ranged from 0.4 to 0.6) and between the influence of
204 rivers and distance to deep water (pairwise correlation of 0.48). All GIS analyses were
205 performed using the ESRI ArcGIS (ArcMap 10.2.1 and Spatial Analyst extension).
206

207 Species distribution models

208

209 Traditional examples of species distribution models are generalized linear and
210 additive models (Guisan et al. 2002; Gelfand et al. 2006). Additionally, a wide variety of
211 other models have been proposed (e.g. Elith et al. 2006; Shelton et al. 2014; Thorson et al.
212 2015), and some of the most popular are non-parametric (Austin 2007; Elith et al. 2008).
213 Here, we built Bayesian species distribution models using Gaussian processes (GPs), as
214 proposed by Vanhatalo et al. (2012). GPs are stochastic processes that define the probability
215 distribution over functions and can be seen as an extension to linear and additive models
216 (Rasmussen 2004; Vanhatalo et al. 2012). They have received considerable interest in many
217 fields of science in recent years due to their semi-parametric nature, which allows flexible
218 and versatile modeling.

219 We modeled the conditional distribution for the number of larvae, $y(s,t)$, at
220 sample location s (coordinates in kilometers) in year t with a negative binomial distribution

221 $$y(s,t)|f(s,t),r \sim \text{Negative} - \text{Binomial}\left(z(s,t)e^{f(s,t,x_s)}, r\right),$$

222 where $z(s,t)$ is the corresponding sampling effort, the latent function $f(s,t,x_s)$ corresponds
223 to the logarithm of the larval density, x_s is the spatially indexed vector of D covariates (see
224 Table 1), and r is the overdispersion parameter. We parameterized the negative binomial as
225 in Vanhatalo et al. (2013) with a quadratic mean-variance relationship so that mean
226 $E[y(s,t)] = z(s,t)e^{f(s,t,x_s)}$ and variance $Var[y(s,t)] = E[y(s,t)] + E[y(s,t)]^2/r$. Hence,
227 increasing r corresponds to decreasing variance, and at the limit, as r approaches infinity, the
228 negative binomial approaches a Poisson distribution. Before modeling, we scaled all the
229 covariates to have a unit standard deviation and zero mean according to the observed values.

The larval density should be interpreted as an index proportional to the true density, since our model does not account for the catchability of the used sampling gear, and it represents the expected (average) number of larvae per cubic meter of water at a particular location and time. The catchability of our sampling gear was mostly influenced by the weather conditions during the sampling occasions. Special attention was paid to standardizing these conditions as well as possible, and there were no systematic variations in the sampling conditions between different areas (see also Study area and data collection section). Hence, it is reasonable to assume that catchability did not vary systematically. However, due to random variation in the sampling conditions, there might still be random variation in catchability. In addition to other sources of extra variation, the spatial and spatio-temporal random effects account for spatially correlated and the overdispersion in negative-binomial distribution for uncorrelated variation in catchability. Overdispersion may arise from various factors in addition to the variation in catchability, including a spatially aggregated distribution of individuals (Lindén and Mäntyniemi 2011).

We assumed that the latent function is additive so that

$$f(s,t,x_s) = \alpha + \sum_{d=1}^{D} g_d(x_{s,d}) + h(x_s) + \rho(s) + \phi(s,t).$$

Here, α is the intercept, $g_d(\cdot)$ is a univariate function of the d^{th} covariate, $h(x_s)$ is a function of interactions between all the covariates, $\rho(s)$ is a spatial random effect, and $\phi(s,t)$ is a spatio-temporal random effect. Hence, the model is essentially a generalized additive model with random effects (Hastie and Tibshirani 1990) and the motivation for the chosen model structure is the following. The intercept describes the average density of larvae across the study area. The univariate function, $g_d(\cdot)$, corresponds to the independent effect of a covariate *d* and, hence, describes the average relative change in density with respect to that covariate across the whole study area. The function of interactions governs the joint effect of

all the covariates. The lower order interactions were left out in order to reduce the complexity of the model (see e.g. Plate 1999). This choice was justified, since it was *a priori* likely that the independent effects would be stronger than interactions, and because our prior for $h(x_s)$ shrinks the effects of covariates towards zero if the data do not support the full order of interactions. The spatial random effect captures spatial autocorrelation, which causes neighboring areas to have similar larval densities because of, for example, associations unexplained by the available covariates (Latimer et al. 2006; Elith and Leathwick 2009). Similarly, the spatio-temporal random effect adjusts for annual variation in density that cannot be described by the temporally constant covariates.

Following Vanhatalo et al. (2012), we gave a Gaussian prior for the intercept $\alpha \sim N(0, \sigma_\alpha^2)$ and Gaussian process (GP) priors for all the latent functions

$$g_d(x_{s,d}) \sim GP\left(0, k_{g_d}(x_{s,d}, x_{s',d} | \theta_{g_d})\right)$$

$$h(x_s) \sim GP\left(0, k_{\mathrm{h}}(x_s, x_{s'} | \theta_{\mathrm{h}})\right)$$

$$\rho(s) \sim GP\left(0, k_\rho\left(s, s' | \theta_\rho\right)\right)$$

$$\phi(s,t) \sim GP\left(0, k_\phi\left((s,t),(s',t') | \theta_\phi\right)\right).$$

GP is a stochastic process that defines the probability distribution over functions (Gelfand et al. 2010; Rasmussen and Williams 2006). It is defined by a mean function, here zero, and a covariance function, e.g., $k_{g_d}(x_{s,d}, x_{s',d}) = Cov\left(g_d(x_{s,d}), g_d(x_{s',d})\right)$, which determines the properties of the process, such as how much and how fast (smoothness) the function varies along a covariate. Here, $x_{s,d}$ and $x_{s',d}$ are the d^{th} covariate at locations s and s', respectively.

We used the neural network covariance function for each univariate function, $k_{g_d}(x_{s,d}, x_{s',d} | \theta_{g_d}) = \frac{2}{\pi} \sin^{-1}\left(\frac{2\tilde{x}_{s,d}^T \theta_{g_d} \tilde{x}_{s',d}}{\sqrt{\left(1+2\tilde{x}_{s,d}^T \theta_{g_d} \tilde{x}_{s,d}\right)\left(1+2\tilde{x}_{s',d}^T \theta_{g_d} \tilde{x}_{s',d}\right)}}\right)$ (Rasmussen and Williams

2006), where $\tilde{x}_{s,d} = [1, x_{s,d}]$ and $\theta_{g_d} = \text{diag}(\sigma^2_{g_d,0}, \sigma^2_{g_d})$. The parameters $\sigma^2_{g_d}$ and $\sigma^2_{g_d,0}$ respectively govern how smooth the function is along x_d and its offset from zero, so that the larger the variance parameters are, the more quickly the function varies. The neural network covariance function gives rise to non-linear and non-stationary random processes whose expected value outside the data range stabilizes (approximately) to the level at which it was at the end of the data range (Vanhatalo et al. 2012). These properties are justified, since it was *a priori* likely that abundance responds to covariates non-linearly, and due to the sampling design, the density is not expected to change radically from the level at the end of the data range when moving outside the data range.

The interactions between covariates were modeled by giving $h(x_s)$ a squared exponential covariance function $k_h(x_{s,d}, x_{s\prime,d}|\theta_{\text{h}}) = \sigma_h^2 e^{-\sum_{d=1}^{D} w_d^2 (x_{s,d} - x_{s\prime,d})^2/2}$, where $\theta_{\text{h}} = [\sigma_h^2, w_1, \ldots, w_D]$, w_d is the weight (inverse length scale; Rasmussen and Williams 2006) along covariate *d* and σ_h^2 is the process variance (magnitude). The weight governs how fast the function varies along $x_{s,d}$ and hence its effect in the interaction term. The effect of a covariate in the interaction term vanishes when the respective weight approaches zero. The magnitude governs the importance of the interaction term relative to other terms.

For the spatial random effect, we used an exponential covariance function $k_\rho(s, s') = \sigma_\rho^2 \text{e}^{-\sqrt{\sum_{i=1}^{2}(s_i - s\prime_i)^2/\lambda_i^2}}$, and for the spatio-temporal random effect we used a separable covariance function with an exponential form for both the space and the time components, so that $k_\phi((s,t),(s',t')) = \sigma_\phi^2 \text{e}^{-\sqrt{\sum_{i=1}^{2}(s_i - s\prime_i)^2/l_i^2}} \text{e}^{-|t-t'|/l_3}$. The length-scale parameters govern the autocorrelation length of the GP along longitude (λ_1, l_1), latitude (λ_2, l_2) and time (l_3), so that the correlation between two locations drops below 5% of its maximum when these locations are further than approximately three times the length scale

299 apart. The variance parameters σ_ρ^2 and σ_ϕ^2 govern the magnitude of the process variation. The
300 exponential covariance function leads to a stationary process in time and space, and is a
301 common choice when modeling spatial processes (Gelfand et al. 2010).
302 We used log-uniform priors for the variance parameters σ_ρ^2, σ_ϕ^2, σ_h^2 and
303 $\{\sigma_{g_d,0}^2, \sigma_{g_d}^2\}_{d=1}^{D}$ and weakly informative half Student-*t* priors (Gelman 2006) for the other
304 hyper-parameters. For weights w_d and the temporal length scale, l_3, we used four degrees of
305 freedom and scale one in the half Student-*t* prior, and for the spatial length scales λ_1, λ_1, l_1,
306 l_2 we used four degrees of freedom and scale 100. All the priors are summarized in Table 2.
307 Since the chosen priors have most of their mass near zero, they favor rigid functional forms
308 (that is, functions that vary slowly along the covariates) with a low order of interactions and a
309 short autocorrelation length in the random effects. We conducted a sensitivity test for the
310 priors by increasing the scale of the half Student-*t* priors by ten-fold and could conclude that
311 the results were not sensitive to the chosen priors.
312
313 Inference, prediction, and model assessment
314
315 We built and inferred one model for each of the four target species. We applied
316 Bayes' theorem and calculated the posterior distribution of all model parameters and latent
317 functions using the expectation propagation and Markov chain Monte Carlo algorithms
318 implemented in the Matlab toolbox GPstuff (Vanhatalo et al. 2013; Appendix A1)[1]. We
319 conducted convergence diagnostics for the Markov chains and used the posterior predictive
320 check (Gelman et al. 2013) for model validation by simulating replicate measurements from

[1] The code to implement the models is given in the Supplementary material.

321 the posterior predictive distribution of each model and compared the samples with the
322 measured data. We also assessed the importance of the spatial and spatio-temporal random
323 effects by comparing our model with similar models without the random effects. See
324 Appendix A1 for details.

325 The full set of environmental covariates fell into seven groups of covariates that
326 were *a priori* potentially good proxies for the essential environmental characteristics of the
327 reproduction habitats. Three of the groups contained several similar covariates at varying
328 spatial scales (Table 1). For example, varying the diameter from 3 km to 15 km for the circles
329 in which the shoreline density was calculated corresponded to a change from a local to a
330 more global shoreline density index. On the other hand, changing from the distance to 10-m-
331 deep water to the distance to 30-m-deep water changed the focus from shallow waters to
332 deeper waters, since in the coastal region of the northern Baltic Sea, the distance from 10-m-
333 deep to 30-m-deep waters may be so large that the latter is not descriptive in the shallowest
334 regions. For each species, we selected the best environmental covariate from each of the
335 groups of covariates according to the leave-one-out cross-validated log predictive density
336 (Vehtari and Ojanen 2012). The final analyses were conducted with the reduced covariate set,
337 which made the interpretation of the results easier.

338 After solving for the posterior, we calculated the marginal posterior predictive
339 distribution of the latent function $f(s, t, x_s)$ and, hence, larval density in the surface water
340 layer of all grid cells in the entire study area. Since we had the spatio-temporal component in
341 our model, we predicted the mean density over the survey years as detailed in Appendix A1.
342 For each species, we present the larval density and its coefficient of variation over the study
343 area. We also approximated the total number of larvae in the surface water layer per sea area
344 and across the whole study area from the sum of the predictive densities in grid cells in an

area multiplied by the water volume of the surface water layer up to the depth of 1.5 m in a grid cell (i.e., 1.5 x 50 x 50 m^3). Since we had over 12 million grid cells in the whole study area, we needed to approximate the posterior distribution of the sum as described in Appendix A1.

In order to study the relative importance of different parts of the study area for fish reproduction, we classified the total area into not suitable, suitable, and important areas. Each grid cell was classified as not suitable if the expected probability for zero observations in a sample of three transects (the average number of transects per sample) was more than 50%. This limit corresponds to using an occurrence model to classify areas as not suitable based on a 50% cut-off value. Next, in order to emphasize the most important fish reproduction areas, we further divided the remaining grid cells into two classes. The important grid cells are those that were in the smallest subset of grid cells whose expected cumulative number of larvae was 80% of the total expected number of larvae in all grid cells that had a presence probability of 50% or more. The rest of the grid cells were classified as suitable. The rationale for this division is the following. Knowledge of potential species reproduction areas (areas with 50% or more probability of larval presence) is necessary for coastal spatial planning and management. However, it is not sufficient information for efficient management, since the larval density in these areas may vary considerably, and the importance of these areas for reproduction at the population level may thus range from very low to very high. Hence, the expected number of larvae produced by an area provides a more informative summary for management, since it is directly related to that area's expected utility for fish production. Here, we chose the cut-off value for demonstrative purposes, and other values could be more justified in specific management applications.

Since the latent function includes interactions between covariates, its response along individual covariates may vary across locations (Vanhatalo et al. 2012). Hence, in order to examine the effect of covariates on larval density, we visualized the expected, zero-centered change in the log density along each covariate and variation in it over the training data locations. See Appendix A1 for details.

Results

Model assessment and posterior inference

All models performed well according to the posterior predictive checks. Table 3 summarizes the posterior distribution of the spatial random effects, the overdispersion parameter, and the variance of the interaction term. The posterior mean of the intercept term corresponded to an average of 2.3×10^{-2} larvae per m^3 for perch, 1.4×10^{-3} larvae per m^3 for pikeperch, 6.3×10^{-2} larvae per m^3 for Baltic herring, and 3.6×10^{-2} larvae per m^3 for smelt. In perch, herring, and smelt models, there was clear overdispersion compared to a standard Poisson model. In the pikeperch model, the overdispersion parameter was higher, but on the other hand, the length scales of the spatio-temporal random effect in this model were considerably smaller than in other models. As the length scales approach zero, this random effect approaches spatially independent overdispersion and takes essentially the same role as the overdispersion parameter. According to the spatial length scales, the spatial autocorrelation in the random effects vanished in tens of kilometers. Hence, compared to the scale of the whole modeled area, the random effects described local corrections to density predictions made by the covariates only. According to the temporal length scales of the

392 spatio-temporal random effects, the spatio-temporal correlations dropped to approximately
393 20% of their maximum between consecutive years and practically to zero correlation after
394 two years. Hence, there were no temporal trends in larval abundances.
395 According to the cross-validation tests, the models worked significantly better
396 than otherwise similar models without any random effects and practically as well as or better
397 than otherwise similar models only having either one of the random effects. Moreover, once
398 random effects were dropped from a model, its overdispersion parameter tended to decrease,
399 which indicates that (part of) the variation captured by the random effects was then
400 transferred to the overdispersion. See Appendix A1 for the comparison results.
401 Figure 2 shows the posterior predictive response of log density along
402 environmental covariates for each species. All the responses were mostly additive, since there
403 was only moderate variation in the responses across the study region. A change in log density
404 by one unit corresponded to a 2.7-fold increase in the density. Hence, the most significant
405 covariate effects, with a change in log density by 3–4 units, corresponded to a 20–50-fold
406 increase in the larval density. The responses of larval densities along environmental
407 covariates varied between the species. Perch had negative responses to an increasing depth,
408 average depth and exposure and positive responses to an increasing distance to deep water
409 (10 m), the influence of rivers, and the cumulative spring temperature. Pikeperch had strong
410 negative responses to an increasing average depth, shoreline density, and exposure, and
411 strong positive responses to an increasing distance to deep water (10 m) and the cumulative
412 spring temperature. Baltic herring had a negative response to the distance to deep water (20
413 m) and strong positive responses to an increasing average depth, shoreline density, and
414 exposure. The response of Baltic herring to an increasing cumulative spring temperature was
415 positive, with a peak at 1200 day-degrees, and at higher cumulative temperatures it turned

negative. Smelt had strong negative responses to an increasing average depth, negative responses to shoreline density and exposure, and positive responses to an increasing distance to deep water (30 m), the influence of rivers, and the cumulative spring temperature.

Larval density predictions

Larval habitats for pikeperch, perch, and smelt were characterized as shallow, sheltered and, thus, areas that warmed relatively rapidly, which were most often found in the inner archipelago, frequently close to river mouths. A somewhat opposite pattern was typical for Baltic herring larval habitats, which were characterized as more exposed areas with a lower cumulative spring temperature compared to other studied species (Figs 2 and 3). Pikeperch had the most and the Baltic herring the least limited environmental requirements of the studied species, concerning the environmental covariates used here.

Figure 3 illustrates the predicted larval density classified into three classes: not suitable, suitable and important. Figure 4 summarizes the posterior predictive median and coefficient of variation of the larval density, and Table 4 summarizes the total number of larvae and areas suitable for reproduction across the study region and the five sea areas. Baltic herring had the highest predicted total number of larvae of the target species in the studied area; the predicted total number of larvae as a percentage of the total number of Baltic Herring larvae was 17.9% for perch, 6.2% for pikeperch, and 67.8% for smelt. The total area suitable for larval production was largest for Baltic herring, covering 99.8% of the studied coastal area. The most limited larval production area (3.7%) was recorded for pikeperch. The proportion of the studied coastal area suitable for larval production was 13.7% for perch and 22.5% for smelt. There was, however, variation in the species-specific distribution of larval

production areas between the five studied sea areas (Table 4); larval production areas for perch and smelt were proportionally larger in the northern parts of the study area (I–III for perch, I for smelt), whereas larval production areas for pikeperch and Baltic herring were proportionally larger in the southern parts of the study area (IV–V).

The important habitats (those that accounted for 80% of larval production) were more limited than the suitable larval habitats, comprising 3.0% of the studied sea area for perch, 1.4% for pikeperch, 52.9% for Baltic herring, and 4.4% for smelt (Table 4). The spatial focus of the important habitats also varied, reflecting the same south–northward pattern seen for the total larval production areas (Fig. 3).

Discussion

By modeling and mapping the reproduction habitats of four common commercially and ecologically important fish species in the northern Baltic Sea, we demonstrated that very limited coastal areas can be crucial for fish reproduction. The availability of suitable larval reproduction habitats is not necessarily a good indicator of important fish reproduction areas, since some suitable habitats may contribute orders of magnitude more to the total larval production than others. Therefore, abundance models should be preferred over occurrence models when studying the reproduction habitats of fish and their quality and impact on total fish production. Our results support the recent findings of Johnston et al. (2015) that abundance models are more accurate and thus preferable for both aggregated and non-aggregated species.

High-resolution prediction maps are a powerful tool that aids visual communication. However, scaling and setting the right cut-off values for map visualization

464 are fundamentally important in order to quantify the interpretation of the maps, prevent
465 misunderstanding, and enable the comparison and value judgment of different coastal sea
466 areas for larval fish production. Visualizing maps, as proposed in this work, very clearly
467 show that the most productive larval habitats can be very limited compared to the entire
468 suitable reproduction habitats of a species; the areas expected to produce 80% of the species-
469 specific larval production (important areas) were two to five times more limited than the
470 entire larval production areas (suitable areas), and varied between species from 1.4% to
471 52.9% of the total study area. This information should be taken into account when planning
472 management and conservation measures. However, the 80% cut-off level in this work was
473 chosen for demonstrative purposes and, depending on a species, another level could be more
474 justified. For example, when analyzing healthy and balanced fish stocks that allow for
475 exploitation without risk of stock depletion, a lower cut-off level (<80% of the cumulative
476 larval production) could be enough to present the assumedly extensive larval production
477 habitats. On the other hand, some endangered fish stocks could demand a much higher cut-off
478 level (>80% of the cumulative larval production) in order to apply a precautionary approach
479 when focusing conservation acts. Hence, the cut-off level for the important reproduction
480 areas should ideally be chosen in parallel with stock assessment and reflect the management
481 and conservation objectives. Moreover, in some applications, we could be interested in a
482 more precautionary summary than the expected number of larvae. For example, the important
483 area could have a cut-off value ensuring that the total number of larvae in that area is greater
484 than a certain percentage of the total number of larvae in the whole study area with a
485 probability greater than, for example, 0.9.
486 We found large differences in the spatial larval habitat distribution between the
487 four studied fish species. The response of Baltic herring to environmental covariates, i.e.

488 environmental requirements, was the least limited of the studied species, and its larval
489 production area was the widest. The pikeperch, on the other hand, is an example of a species
490 with very strict environmental requirements in the reproductive stage (Sundblad et al. 2014;
491 Veneranta et al. 2011), and its total reproduction area was accordingly the most limited. The
492 specific ecological habitat requirements of each species were also reflected in the responses
493 of larval densities to the environmental covariates chosen for the species-specific models. For
494 example, both pikeperch and perch larvae were most abundant in areas that had a high
495 cumulative spring temperature, which supports the finding that the year-class strength of both
496 pikeperch and perch is known to largely depend on temperature (Kjellman et al. 2003;
497 Pekcan-Hekim et al. 2011; Lehtonen et al. 1996). Moreover, the covariates chosen for the
498 pikeperch model describe very local aspects in the inner archipelago, whereas the covariates
499 chosen for the herring model describe broader and more pelagic aspects. Overall, the results
500 emphasized the importance of the shallow parts of the coastal area, but when interpreting the
501 results one has to keep in mind that the field survey was only conducted in the surface water
502 layer.

503 The Baltic herring had the highest predicted total number of larvae according to
504 our results. This was expected, since it has the highest stock size of the studied species and is
505 the most important species for fisheries in the northern Baltic Sea (Söderkultalahti 2015). The
506 Baltic herring is a pelagic species that is known to reproduce over a large area and during a
507 time period of several months in spring and early summer (Parmanne et al. 1994; Fey 2001;
508 Hakala et al. 2003). Perch, pikeperch, and smelt, on the other hand, are strictly coastal species
509 with specific and rather similar reproductive requirements and a reproductive period of some
510 weeks (Snickars et al. 2010; Sundblad et al. 2014). Therefore, the suitability of the used field
511 survey and modeling methods probably varied between species. Firstly, sampling should

optimally have been carried out during the whole summer in order to cover several reproductive cohorts and enable modeling of the length of the reproduction season for each species. However, this was not feasible in our survey program, and our model does not therefore take into account the lengths of the reproductive seasons nor the number of cohorts; hence, the total numbers of larvae represent the numbers of larvae produced by those cohorts that our survey covered during the reproduction season. Secondly, only the surface water layer was sampled and modeled here. Larval perch, pikeperch, and smelt are known to be abundant in the surface water layer (Urho et al. 1990), but Baltic herring larvae are also found in deeper water layers (Sjöblom and Parmanne 1978). Therefore, the model should have taken into account the entire water layer in which larvae are present in order to compare the total numbers of larvae between species. Since our sampling did not provide information on the distribution depth, we restricted our study to the surface water layer and assumed that the distribution depth does not differ significantly between areas. According to earlier studies (Parmanne and Sjöblom 1988), this assumption is reasonable. Thirdly, our model did not explicitly account for variation in catchability, but the modeled density accounted for both catchability and the total abundance of larvae. Hence, systematically varying catchability would introduce bias in our density estimates. However, we do not expect the catchability to have varied systematically between areas, since the weather conditions during the surveys were standardized as well as practically possible. Moreover, the catchability was not expected to differ significantly between pikeperch, perch, and smelt. However, according to the posterior distributions of spatial and spatio-temporal random effects and the overdispersion parameter, the overdispersion compared to the expected density (that is, extra uncertainty) was significant for all species. This overdispersion is expected to partly arise from varying catchability due to weather and other sampling conditions. Therefore, the results presented

here are most robust when examining regional differences in species-specific distribution areas and densities and, unfortunately, the quantitative comparison of the total number of larvae between the studied species is only indicative between perch, pikeperch, and smelt and not possible between herring and other species. It is also important to keep in mind that we sampled early-stage fish larvae, which still have many bottlenecks to survive before they recruit to the adult population (Miller et al. 1988; Myers 1998).

The distribution of species-specific reproduction habitats and species abundances are not static over time, and temporal changes may reduce the long-term generality of the habitat and abundance predictions. Matching the field sampling with the occurrence of early-stage larvae is also challenging, producing uncertainty in the probability of detection. Moreover, constructing good environmental covariates is difficult, and GIS-based environmental covariates can never encode all essential abiotic aspects related to species distributions (Elith et al. 2006). We have addressed these challenges in both the data collection and modeling. The temporal fluctuations were accounted for by using field survey data from multiple years (2007–2014), which allowed us to model the average distribution of reproduction habitats and the average density over those years. The sampling was performed multiple times each year so that the probability of matching it with the presence of early-stage larvae was increased. In constructing the environmental covariates, we used only general environmental descriptors such as depth to increase the generality of the predictions, as suggested by Sundblad et al. (2014), among others. The annual fluctuations and possible time mismatch in sampling were also explicitly modeled by the spatio-temporal random effects component. Moreover, we included the spatial random effect in our model to account for static patterns in data that were not explained by our covariates. According to the results, the random effects improved the model performance compared to otherwise similar models

560 without the random effects (see Appendix A1). Hence, the inclusion of the random effects
561 was justified. If *a priori* justified, we could also model multiple spatial processes at different
562 scales with a different choice of the covariance functions, such as an additive covariance
563 function with short and long length scales (Vanhatalo and Vehtari 2008).
564 GP formalism gives considerable freedom in how to choose the covariance
565 structure of the predictive model for the covariates (Vanhatalo et al. 2012). Here, we used an
566 additive structure that included non-linear univariate terms and a function with interactions.
567 We used neural-network covariance functions for the univariate terms, since they were shown
568 to work well in extrapolation by Vanhatalo et al. (2012). The squared exponential covariance
569 function, on the other hand, is a standard choice to model full interactions (see e.g.
570 Rasmussen and Williams 2006). Our choice of covariance functions proved to be justified
571 here, since all the responses were non-linear and the interactions were rather weak. The
572 models also performed well in the posterior predictive checks. However, the interpolation and
573 extrapolation behavior of a GP depend on the chosen covariance function (Vanhatalo et al.,
574 2012). Some covariance functions, such as the commonly used squared exponential, behave
575 similarly to splines (which are often used in generalized additive models) so that they
576 typically perform well when predicting within the data range (interpolation). However, when
577 extrapolating the prediction outside the data range, the result may be unfavorable, since
578 predictions approach the prior mean (that is, zero). The neural network covariance function
579 works differently by allowing non-linear responses and extrapolations that follow the level at
580 which the predictive function is at the end of the data (see Appendix A1 and Figure A1).
581 However, if we had strong prior knowledge on the likely response, we could describe this
582 with a parametric function, such as a linear, bell shaped or, for instance, Michaelis-Menten
583 functional form (Vanhatalo et al., in press) and use GPs to model possible discrepancies from

584 this parametric form. We chose the environmental variables based on their biological
585 justification and did not transform them in order to remove collinearity, because such
586 transformations would obscure the interpretation of the responses. Collinearity is not a
587 problem when predicting the larval distribution. Compared to prediction with one covariate,
588 in case of strong collinearity between two or more covariates, the predictive contribution is
589 simply divided between the correlated covariates. However, as in (generalized) linear and
590 additive models, collinearity is a challenge when inferring the responses along covariates. In
591 order to remedy this, the hyperparameters of the predictive functions were given weakly
592 informative priors, which prefer constant functions. Hence, in the case of strong collinearity,
593 the response along the "weaker" covariates will be shrunk towards zero, whereas the
594 covariates that explain data better should have a stronger response (see also Simpson et al.
595 2015 for a more general discussion on penalized complexity priors). However, our prior
596 structure did not strictly promote sparsity, and theoretically or empirically justified general
597 rules for choosing the covariance functions for the predictive GP models and priors for their
598 hyperparameters still provide room for future research.
599 The methods presented here provide concrete support for environmental
600 management and the spatial planning of coastal and marine areas by providing a means to
601 prioritize areas with a high production potential (abundance) over areas that are suitable for
602 reproduction but do not significantly contribute to larval production. For example, the results
603 presented here aid in the implementation of the EU Maritime Spatial Planning directive and
604 local dredging permission procedures in Finland to focus on the most important areas from
605 the perspective of larval production. Fisheries stock assessment and management could also
606 benefit from this type of approach, since the results for larval abundance could be used to
607 describe the reproductive potential of a fish stock, as has been conducted for Baltic Salmon

608 (Kuikka et al. 2014), which would not be possible with presence/absence models. Regarding
609 their short-term utilization, the results of this study will help in the implementation of the new
610 Finnish Fishing Act (enacted on January 1st, 2016) which involves changes in the spatial
611 organization of fisheries management in terms of utilization and conservation planning. The
612 implementation of the new law requires detailed information, among others, on fish
613 production areas. Moreover, scientific knowledge of the distribution of fish stocks and
614 important production areas is needed to inform policy makers about the best sustainable
615 management practices and to assess the current fisheries management policies in general.
616 Habitat protection is a strategy often proposed in fisheries and environmental
617 management to help maintain viable populations of exploited or endangered species. Besides
618 habitat quality, habitat connectivity is also considered an important characteristic in the
619 protection of essential coastal habitats (Halpern et al. 2005; Lipcius et al. 2008). In this study,
620 we have shown that species distribution models providing high-resolution predictions for
621 larval density on a geographically wide scale can be used to numerically compare and value
622 different sea areas for larval fish production, and therefore provide easy-to-interpret maps for
623 management and coastal and marine spatial planning purposes. Sundblad et al. (2014) have
624 suggested that a substantial proportion of the potential production of adult fish can be
625 estimated by mapping the distribution of essential fish habitats, since habitat bottlenecks in
626 the early life-stages limit the abundance of later adult stages of predatory fish. Here, we
627 showed that the production of fish stocks can be concentrated in spatially extremely limited
628 areas compared to the suitable production areas. Hence, the total production potential
629 (abundance) of an area should be taken into account in, for example, marine spatial planning.
630 Future efforts should focus on linking this modeling and mapping approach to catches to

study the link between essential habitats and stock assessment of the most important coastal commercial fish species.

Acknowledgements

The authors thank the field staff of Luke who took part in the extensive larval fish survey and Prof. Sakari Kuikka, Dr Antti Lappalainen, Dr Mika Rahikainen, and two anonymous reviewers for valuable comments on the manuscript. The authors also thank Elina Virtanen from the Finnish Inventory Programme for Marine Underwater Environment (VELMU), the Finnish Environment Institute (Syke), for providing the depth data. Meri Kallasvuo and Lari Veneranta were funded by the Ministry of Agriculture and Forestry Finland / VELMU programme (2502/311/2012) and by the Strategic Research Council of the Academy of Finland / SmartSea (grant 292985). Jarno Vanhatalo was funded by the Academy of Finland (grants 266349 and 292985) and Research Funds of the University of Helsinki.

References

Aneer, G. 1989. Herring (*Clupea harengus* L.) spawning and spawning ground characteristics in the Baltic sea. Fish. Res. **8**: 169-195.

Austin, M. 2007. Species distribution models and ecological theory: A critical assessment and some possible new approaches. Ecol. Model. **200**: 1-19.

Benaka, L. 1999. Fish habitat: Essential fish habitat and rehabilitation. American Fisheries Society, Symposium 22, Connecticut.

Cross, J.N., Brown, D.W., and Kurland, J.M. 1997. Essential fish habitat: A new fisheries management tool. ICES council meeting papers, Copenhagen, Denmark.

Elith, J., and Leathwick, J.R. 2009. Species distribution models: Ecological explanation and prediction across space and time. Annu. Rev. Ecol. Evol. Syst. **40**: 677-697. doi: http://www.annualreviews.org/doi/abs/10.1146/annurev.ecolsys.110308.120159 .

Elith, J., Graham, C.H., Anderson, R.P., Dudik, M., Ferrier, S., Guisan, A., Hijmans, R.J., Huettmann, F., Leathwick, J.R., Lehmann, A., Li, J., Lohmann, L.G., Loiselle, B.A., Manion, G., Moritz, C., Nakamura, M., Nakazawa, Y., Overton, J.M.C., Peterson, A.T., Phillips, S.J., Richardson, K., Scachetti-Pereira, R., Schapire, R.E., Soberon, J., Williams, S., Wisz, M.S., and Zimmermann, N.E. 2006. Novel methods improve prediction of species' distributions from occurrence data. Ecography **29**(2): 129-151. doi: 10.1111/j.2006.0906-7590.04596.x.

Elith, J., Leathwick, J.R., and Hastie, T.R. 2008. A working guide to boosted regression trees. J. Anim. Ecol. **77**: 802–813. doi: 10.1111/j.1365-2656.2008.01390.x.

Fey, D.P. 2001. Differences in temperature conditions and somatic growth rate of larval and early juvenile spring-spawned herring from the vistula lagoon, Baltic Sea manifested in the otolith to fish size relationship. J. Fish. Biol. **58**: 1257-1273.

Gelfand, A.E., Holder, M., Latimer, A., Lewis, P.A., Rebelo, A., Silander, J.A., and Wu, S. 2006. Explaining species distribution patterns through hierarchical modeling. Bayesian Anal. **1**: 41-92.

Gelfand, A., Diggle, P.J., Fuentes, M., and Guttorp, P. 2010. Handbook of spatial statistics. CRC press, Miami, USA.

679 Gelman, A. 2006. Prior distributions for variance parameters in hierarchical models.
680 Bayesian Anal. **1**(3): 515-533.
681 Gelman, A., Carlin, J., Stern, H., Dunson, D., Vehtari, A., and Rubin, D. 2013. Bayesian data
682 analysis, third edition. Chapman & Hall / CRC Texts in Statistical Science,
683 Miami, USA.
684 Guisan, A., and Zimmermann, N.E. 2000. Predictive habitat distribution models in ecology.
685 Ecol. Model. **135**(2-3): 147-186.
686 Guisan, A., Edwards Jr, T.C., and Hastie, T. 2002. Generalized linear and generalized
687 additive models in studies of species distributions: Setting the scene. Ecol.
688 Model. **157**(2): 89-100. doi: http://dx.doi.org/10.1016/S0304-3800(02)00204-1.
689 Hakala, T., Viitasalo, M., Rita, H., Aro, E., Flinkman, J., and Vuorinen, I. 2003. Temporal
690 and spatial variation in the growth rates of Baltic herring (*Clupea harengus*
691 *membras* L.) larvae during summer. Mar. Biol. **142**(1): 25-33. doi:
692 10.1007/s00227-002-0933-3.
693 Halpern, B.S., Gaines, S.D., and Warner, R.R. 2005. Habitat size, recruitment, and longevity
694 as factors limiting population size in stage-structured species. Am. Nat. **165**(1):
695 82-94.
696 Hastie, T., and Tibshirani, R. 1990. Generalized additive models. Chapman and Hall,
697 London.Isæus, M. 2004. Factors structuring Fucus communities at open and
698 complex coastlines in the Baltic sea. Department of Botany, Stockholm
699 University, Stockholm.Johnston, A., Fink, D., Reynolds, M.D., Hochachka,
700 W.M., Sullivan, B.L., Bruns, N.E., Hallstein, E., Merrifield, M.S., Matsumoto,
701 S., and Kelling, S. 2015. Abundance models improve spatial and temporal
702 prioritization of conservation resources. Ecol. Appl. **25**: 1749-1756.

703 Juntunen, T., Vanhatalo, J., Peltonen, H. and Mäntyniemi, S. 2012. Bayesian spatial
704 multispecies modelling to assess pelagic fish stocks from acoustic- and trawl-
705 survey data. ICES J. Mar. Sci. **69**: 95-104.
706 Kallasvuo, M. 2010. Coastal environmental gradients. Key to reproduction habitat
707 mapping of freshwater fish in the Baltic Sea [online]. Ph.D. thesis, University
708 of Helsinki. Available from http://urn.fi/URN:ISBN:978-952-10-6392-3.
709 Kjellman, J., Lappalainen, J., Urho, L., and Hudd, R. 2003. Early determination of perch and
710 pikeperch recruitment in the northern Baltic sea. Hydrobiologia. **495**: 181-191.
711 Kuikka, S., Vanhatalo, J., Pulkkinen, H., Mäntyniemi, S., and Corander, J. 2014. Experiences
712 in Bayesian inference in Baltic Salmon management. Stat. Sci. **29**: 42-49.
713 Lappalainen, J., Dörner, H., and Wysujack K. 2003. Reproduction biology of pikeperch
714 (*Sander lucioperca* (L.)) – a review. Ecol. Freshwat. Fish **12**: 95-106.
715 Latimer, A.M., Wu, S., Gelfand, A.E., and Silander, J.A. 2006. Building statistical models to
716 analyze species distributions. Ecol. Appl. **16**: 33-50.
717 Lehtonen, H., Hansson, S., and Winkler, H. 1996. Biology and exploitation of pikeperch,
718 *Stizostedion lucioperca* (L.), in the Baltic Sea. Ann. Zool. Fennici. **33**: 525-535.
719 Lindén, A., and Mäntyniemi, S. 2011. Using the negative binomial distribution to model
720 overdispersion in ecological count data. Ecology **92**(7): 1414-1421.
721 Lipcius, R.N., Eggleston, D.B., Schreiber, S.J., Seitz, R.D., Shen, J., Sisson, M.,
722 Stockhausen, W.T., and Wang, H.V. 2008. Importance of metapopulation
723 connectivity to restocking and restoration of marine species. Rev. Fish. Sci.
724 **16**(1-3): 101-110. doi: 10.1080/10641260701812574.

725 Miller, T.J., Crowder, L.B., Rice, J.A., and Marschall, E.A. 1988. Larval size and recruitment
726 mechanisms in fishes: Toward a conceptual framework. Can. J. Fish. Aquat.
727 Sci. **45**: 1657-1670.
728 Myers, R.A. 1998. When do environment–recruitment correlations work? Rev. Fish Biol.
729 Fisher. **8**: 285-305.
730 Parmanne, R., and Sjöblom, V. 1988. The abundance of spring spawning Baltic herring
731 larvae in the seas around Finland in 1982 and 1983, zooplankton abundance and
732 the herring year-class strength. Finnish Fish. Res. **7**: 1-11.
733 Parmanne, R., Rechlin, O., and Sjöstrand, B. 1994. Status and future of herring and sprat
734 stocks in the Baltic Sea. Dana **10**: 29-59.
735 Pekcan-Hekim, Z., Urho, L., Auvinen, H., Heikinheimo, O., Lappalainen, J., Raitaniemi, J.,
736 and Söderkultalahti, P. 2011. Climate warming and pikeperch year-class catches
737 in the Baltic Sea. Ambio. **40**(5): 447-456. doi: 10.1007/s13280-011-0143-7.
738 Plate, T.A. 1999. Accuracy versus interpretability in flexible modelling: Implementing a
739 tradeoff using gaussian process models. Behaviourmetrika **26**: 29-50.
740 Rasmussen, C.E. 2004. Gaussian processes for machine learning. *In* Machine learning. *Edited*
741 *by* O. Bousquet. Springer-Verlag, Berlin, Heidenberg. pp. 33-71.
742 Rasmussen, C.E., and Williams, C.K.I. 2006. Gaussian processes for machine learning. The
743 MIT Press, Massachusetts, USA.
744 Seitz, R.D., Wennhage, H., Bergström, U., Lipcius, R.N., and Ysebaert, T. 2014. Ecological
745 value of coastal habitats for commercially and ecologically important species.
746 ICES J. Mar. Sci. **71**(3): 648-665. doi: 10.1093/icesjms/fst152.

747 Shelton, A.O., Thorson, J.T., Ward, E.J., and Feist, B.E. 2014. Spatial semiparametric models
748 improve estimates of species abundance and distribution. Can. J. Fish. Aquat.
749 Sci. **71**: 1655-1666. doi:10.1139/cjfas-2013-0508
750 Shpilev, H., Ojaveer, E., and Lankov, A. 2005. Smelt (*Osmerus eperlanus* L.) in the Baltic
751 Sea. Proc. Estonian Acad. Sci. Biol. Ecol. **54**: 230-241.
752 Simpson, D.P.; Rue, H., Martins, T.G., Riebler, A., and Sørbye, S.H. 2015. Penalising model
753 component complexity: A principled, practical approach to constructing priors
754 [online]. Available from: arXiv:1403.4630v4
755 Sjöblom, V., and Parmanne, R. 1978. The vertical distribution of Baltic herring larvae
756 (*Clupea harengus* L.) in the Gulf of Finland. Finnish Fish. Res. **2**: 5-18.
757 Snickars, M., Sundblad, G., Sandström, A., Ljunggren, L., Bergström, U., Johansson, G., and
758 Mattila, J. 2010. Habitat selectivity of substrate-spawning fish: Modelling
759 requirements for the Eurasian perch *Perca fluviatilis*. Mar. Ecol. Prog. Ser. **398**:
760 235-243.
761 Söderkultalahti, P. 2015. Ammattikalastus merellä (Commercial fisheries in the northern
762 Baltic Sea) [online]. Natural Resources Institute Finland. Available from:
763 http://stat.luke.fi/ammattikalastus-merell%C3%A4-2014_fi 16.5.2016.
764 Sundblad, G., and Bergström, U. 2014. Shoreline development and degradation of coastal
765 fish reproduction habitats. Ambio. **43**: 1020-1028. doi: 10.1007/s13280-014-
766 0522-y.
767 Sundblad, G., Bergström, U., Sandström, A., and Eklöv, P. 2014. Nursery habitat availability
768 limits adult stock sizes of predatory coastal fish. ICES J. Mar. Sci. **71**: 672-680.
769 doi: 10.1093/icesjms/fst056.

770 Thorson, J.T., Shelton, A.O., Ward, E.J., and Skaug, H.J. 2015. Geostatistical delta-
771 generalized linear mixed models improve precision for estimated abundance
772 indices for West Coast groundfishes. ICES J. Mar. Sci. **72**: 1297-1310.
773 doi:10.1093/icesjms/fst176
774 Urho, L. 1996: Identification of perch (*Perca fluviatilis*), pikeperch (*Stizostedion lucioperca*)
775 and ruffe (*Gymnocephalus cernuus*) larvae. Ann. Zool. Fenn. **33**: 658-667
776 Urho, L. 2002: Characters of larvae – what are they? Folia Zool. **51**: 161-186.
777 Urho, L., and Hildén, M. 1990. Distribution patterns of Baltic herring larvae, *Clupea*
778 *harengus* L., in the coastal waters off Helsinki, Finland. J. Plankton Res. **12**(1):
779 41-54. doi: 10.1093/plankt/12.1.41.
780 Urho, L., Hildén, M., and Hudd, R. 1990. Fish reproduction and the impact of acidification in
781 the Kyrönjoki river estuary in the Baltic Sea. Environ. Biol. Fishes. **27**: 273-
782 283.
783 Vanhatalo, J. and Vehtari, A. 2008. Modelling local and lobal phenomena with sparse
784 Gaussian processes [online]. Proceedings of the 24th Conference on
785 Uncertainty in Artificial Intelligence, Helsinki. Available at:
786 https://arxiv.org/ftp/arxiv/papers/1206/1206.3290.pdf
787 Vanhatalo, J., Veneranta, L., and Hudd, R. 2012. Species distribution modeling with
788 Gaussian processes: A case study with the youngest stages of sea spawning
789 whitefish (*Coregonus lavaretus* L. s.l.) larvae. Ecol. Model. **228**: 49-58.
790 Vanhatalo, J., Riihimäki, J., Hartikainen, J., Jylänki, P., Tolvanen, V., and Vehtari, A. 2013.
791 GPstuff: Bayesian modeling with Gaussian processes. J. Mach. Learn. Res. **14**:
792 1175-1179. doi: http://arxiv.org/pdf/1206.5754.pdf.

793 Vanhatalo, J., Hosack, G. and Sweatman, H. (In press). Spatio-temporal progression of
794 outbreaks of the crown-ofthorns starfish on the Great Barrier Reef, 1985-2014.
795 J. Appl. Ecol.
796 Vehtari, A., and Ojanen, J. 2012. A survey of Bayesian predictive methods for model
797 assessment, selection and comparison. Stat. Surv. **6**: 142-228.
798 Veneranta, L., Urho, L., Lappalainen, A., and Kallasvuo, M. 2011. Turbidity characterizes
799 the reproduction areas of pikeperch (*Sander lucioperca* (L.)) in the northern
800 Baltic Sea. Estuar. Coast. Shelf Sci. **95**: 199-206.
801 Voipio, A. 1981. The Baltic Sea. Elsevier, Amsterdam, the Netherlands.
802

803 Table 1. Environmental predictor covariates used in species distribution modeling. Range values of the covariates are given for the entire study
804 area.
805

Covariate group	Covariate	Description	Type	Spatial res. (m)	Range	Unit	Source
Depth	depth	Depth from bottom topography	Cont.	20	0.5-275.9	m	Syke
Average depth	dptavg3km	Average depth in a circle of 3 km	Cont.	50	0.5-258.5	m	Luke
	dptavg5km	Average depth in a circle of 5 km	Cont.	50	0.5-251.9	m	Luke
	dptavg10km	Average depth in a circle of 10 km	Cont.	50	1.0-232.8	m	Luke
	dptavg15km	Average depth in a circle of 15 km	Cont.	50	1.3-210.9	m	Luke
Distance to deep	dist10m	Distance to 10 m depth zone	Cont.	50	0-35.4	km	Luke
water	dist20m	Distance to 20 m depth zone	Cont.	50	0-47.7	km	Luke
	dist30m	Distance to 30 m depth zone	Cont.	50	0-85.1	km	Luke

Influence of rivers	river	Square root of inverse distance to nearest river mouth weighted with annual average runoff	Cont.	50	0.1-3.6	index sum	Luke
Shoreline density	shoreline3km	Shoreline length in a circle of 3 km	Cont.	50	0-10.3	m/km^2	Luke
	shoreline5km	Shoreline length in a circle of 5 km	Cont.	50	0-7.5	m/km^2	Luke
	shoreline10km	Shoreline length in a circle of 10 km	Cont.	50	0-5.3	m/km^2	Luke
	shoreline15km	Shoreline length in a circle of 15 km	Cont.	50	0-4.3	m/km^2	Luke
Exposure	exposure	Log10 of wave exposure	Cont.	25	2.1-6.1	$log10(m^2s^{-1})$	Aquabiota
Cumulative spring temperature	tempsum	Cumulative temperature sum from ice-break to July 15	Cont.	50	490.1-3109.2	˚C	Luke

806

807 Table 2. The priors for model parameters. Here, $N(m,\tau)$ is the Gaussian distribution with
808 mean m and variance τ, $\text{Student}_+ - t(\upsilon, m, s)$ is the Student-t distribution restricted on non-
809 zero values with υ degrees of freedom, location m, and scale s, and $\text{Gamma}(\alpha,\beta)$ is the
810 Gamma distribution with shape α and inverse scale β (Gelman et al. 2013).
811

Parameter	Prior
Mean log density (intercept), α	$N(0,10)$
Over dispersion, r	$\text{Gamma}(2,0.1)$
Variance of spatio-temporal component σ_ϕ^2	$p(\sigma_\phi^2) \propto 1/\sigma_\phi^2$
Longitudinal length scale of spatio-temporal component, l_1	$w_d \sim \text{Student}_+ - t(4,0,100)$
Latitudinal length scale of spatio-temporal component,l_2	$w_d \sim \text{Student}_+ - t(4,0,100)$
Temporal length scale of spatio-temporal component, l_3	$w_d \sim \text{Student}_+ - t(4,0,1)$
Variance of spatial component σ_ρ^2	$p(\sigma_\rho^2) \propto 1/\sigma_\rho^2$
Longitudinal length scale of spatial component, λ_1	$w_d \sim \text{Student}_+ - t(4,0,100)$
Latitudinal length scale of spatial component,λ_2	$w_d \sim \text{Student}_+ - t(4,0,100)$
Variance of the interaction term, σ_h^2	$p(\sigma_h^2) \propto 1/\sigma_h^2$
Weights along covariates in the interaction term $\{w_d\}_{d=1}^D$	$w_d \sim \text{Student}_+ - t(4,0,1)$
Variance parameters of the additive functions,	$p(\sigma_{g_d,0}^2) \propto 1/\sigma_{g_d,0}^2$
$\{\sigma_{g_d,0}^2, \sigma_{g_d}^2\}_{d=1}^D$	$p(\sigma_{g_d}^2) \propto 1/\sigma_{g_d}^2$

812

813 Table 3. The posterior median and central 95% credible interval of the overdispersion
814 parameter, variance of the interaction term and parameters of the spatial and spatio-temporal
815 covariance functions.
816

	Perch	Pikeperch	Baltic herring	Smelt
Mean log density (intercept), α	-3.79 (-6.19, -1.40)	-6.59 (-9.16, -4.02)	-2.77 (-4.67, -0.87)	-3.32 (-5.73, 0.90)
Over dispersion, r	1.18 (0.80, 2.25)	11.48 (2.53, 47.97)	1.79 (1.26, 3.02)	2.45 (1.28, 6.84)
Variance of spatio-temporal component σ_{ϕ}^2	6.69 (4.53, 11.08)	0.29 (0.01, 1.47)	2.39 (1.53, 3.80)	2.36 (0.38, 5.23)
Longitudinal length scale of spatio-temporal component, l_1	17.80 (10.47, 31.47)	5.03 (0.42, 26.87)	12.21 (6.76, 24.40)	10.25 (4.60, 28.97)
Latitudinal length scale of spatio-temporal component,l_2	34.11 (17.78, 75.70)	6.88 (0.14, 37.91)	16.93 (9.47, 33.13)	8.53 (2.53, 33.58)
Temporal length scale of spatio-temporal component, l_3	0.88 (0.03, 2.73)	0.70 (0.01, 3.71)	0.61 (0.03, 2.26)	0.66 (0.05, 3.48)
Variance of spatial component σ_{ρ}^2	0.07 (0.00, 1.02)	6.10 (3.43, 13.52)	0.03 (0.00, 0.42)	1.64 (0.00, 4.17)
Longitudinal length scale of spatial component, λ_1	7.34 (0.04, 36.21)	17.10 (9.60, 35.64)	7.59 (0.57, 32.89)	10.05 (1.76, 31.94)

Latitudinal length scale of spatial component,λ_2	7.58 (0.15, 31.39)	18.67 (8.70, 46.88)	8.56 (0.29, 42.25)	14.90 (1.83, 49.51)
Variance of the interaction term, σ_h^2	0.44 (0.01, 2.24)	0.19 (0.00, 2.28)	0.09 (0.00, 0.49)	0.47 (0.01, 3.41)

817

818 Table 4. Expected total number of larvae (95% credible interval), percentage of the studied
819 water area suitable for larvae (suitable areas) and producing 80% of larvae (important areas)
820 by species and sea area (I = Bothnian Bay; II = Quarken area; III = Bothnian Sea; IV =
821 Archipelago Sea; V = Gulf of Finland). The sea areas sum up to the total study area.
822

	Total number of larvae x 10^9 (95% credible interval)	Percentage of water area suitable for larvae	Percentage of water area producing 80% of larvae
Perch			
I	0.48 (0.22, 0.92)	23.32	5.00
II	0.41 (0.21, 0.71)	16.97	7.12
III	0.26 (0.13, 0.47)	18.59	5.41
IV	0.20 (0.11, 0.35)	7.92	0.84
V	0.20 (0.07, 0.48)	12.89	2.40
Total	1.56 (0.89, 2.55)	13.66	3.03
Pikeperch			
I	0.08 (0.003, 0.39)	2.57	1.10
II	0.02 (0.004, 0.05)	1.79	0.42
III	0.03 (0.01, 0.09)	3.35	0.91
IV	0.31, (0.04, 1.16)	3.88	1.80
V	0.10 (0.02, 0.35)	5.71	1.45
Total	0.54 (0.12, 1.56)	3.68	1.37
Baltic herring			
I	0.72 (0.46, 1.06)	99.81	15.71

II	0.50 (0.34, 0.70)	99.87	16.48
III	0.57 (0.41, 0.78)	99.79	24.71
IV	4.93 (3.01, 7.63)	99.87	74.07
V	2.00 (1.12, 3.31)	99.53	78.90
Total	8.72 (5.65, 12.86)	99.79	52.89
Smelt			
I	3.30 (1.22, 7.25)	70.88	12.12
II	0.79 (0.44, 1.32)	25.49	7.43
III	0.74 (0.23, 1.82)	22.27	4.62
IV	0.49 (0.18, 1.06)	5.91	1.12
V	0.58 (0.20, 1.35)	12.34	2.78
Total	5.91 (2.88, 10.81)	22.50	4.44

823

824 Figure legends

825

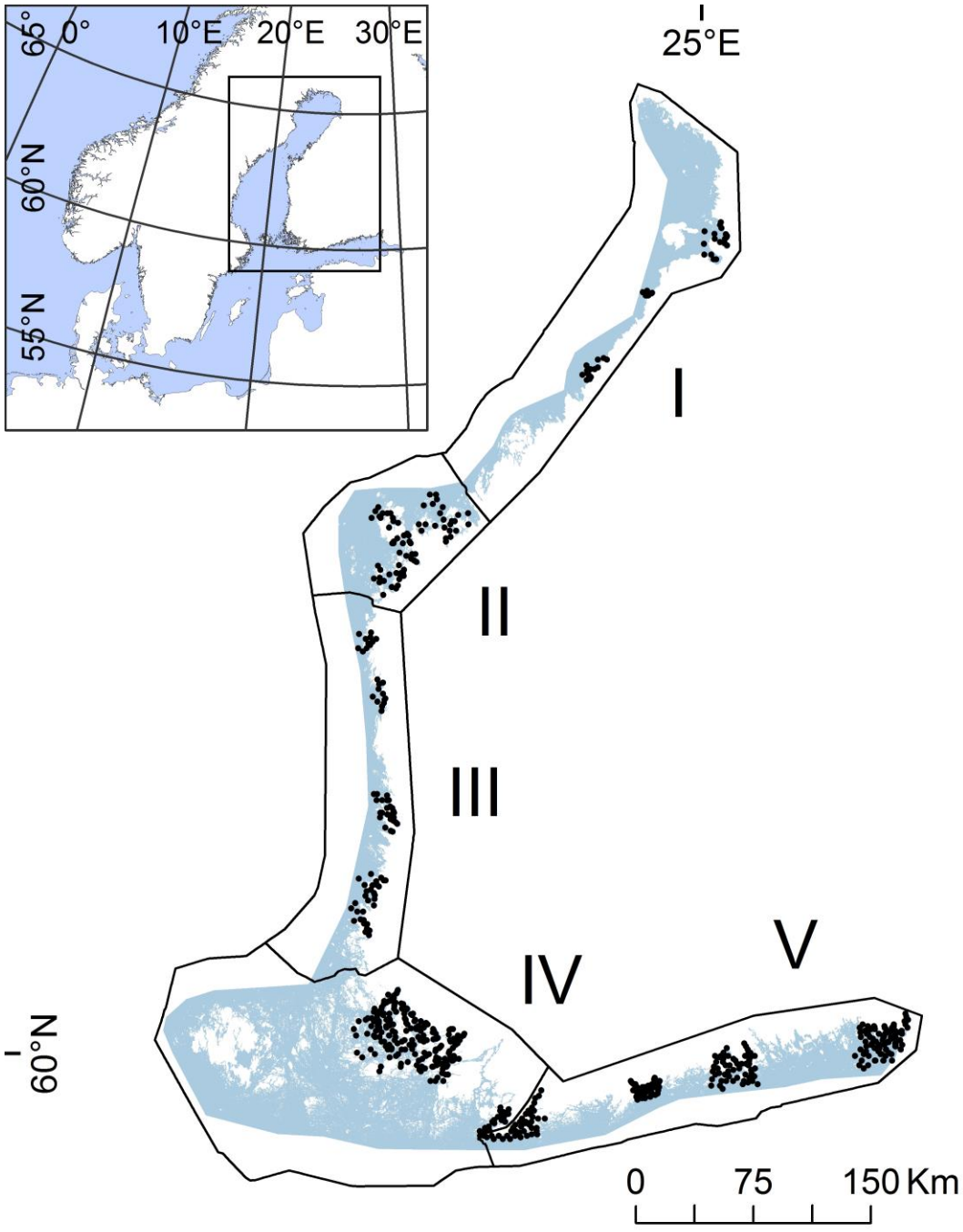

826

827 Figure 1. The study area (grey), larval fish survey sites (black dots) and the sea area divisions

828 (I = Bothnian Bay; II = Quarken area; III = Bothnian Sea; IV = Archipelago Sea; V = Gulf of

829 Finland).

830

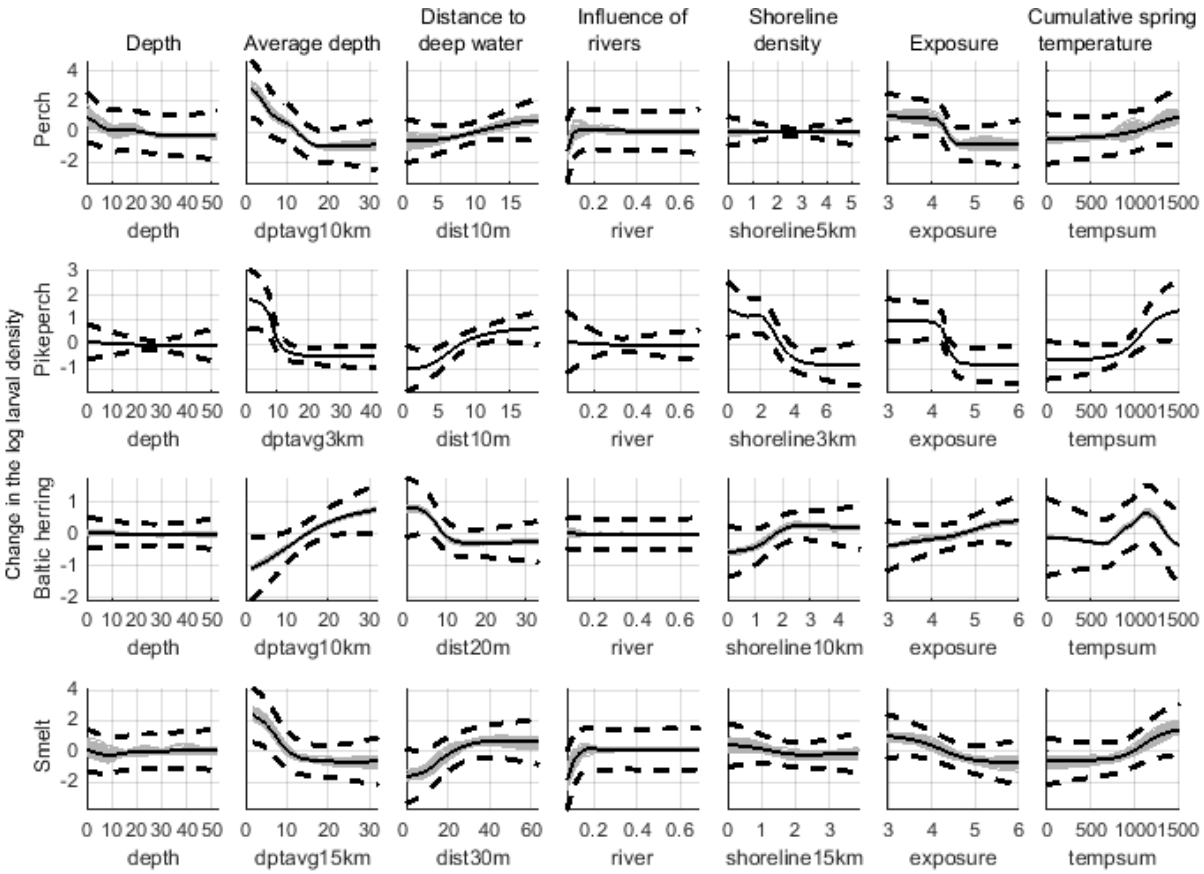

831

832 Figure 2. The response of log-transformed larval density along environmental covariates,
833 shown for the four study species. A change in the log density by one unit corresponds to a
834 2.7-fold increase in the density. The solid and dashed black lines describe, respectively, the
835 average response and the 95% credible interval over all data points. The grey lines show the
836 expected response in 50 randomly chosen locations.

837

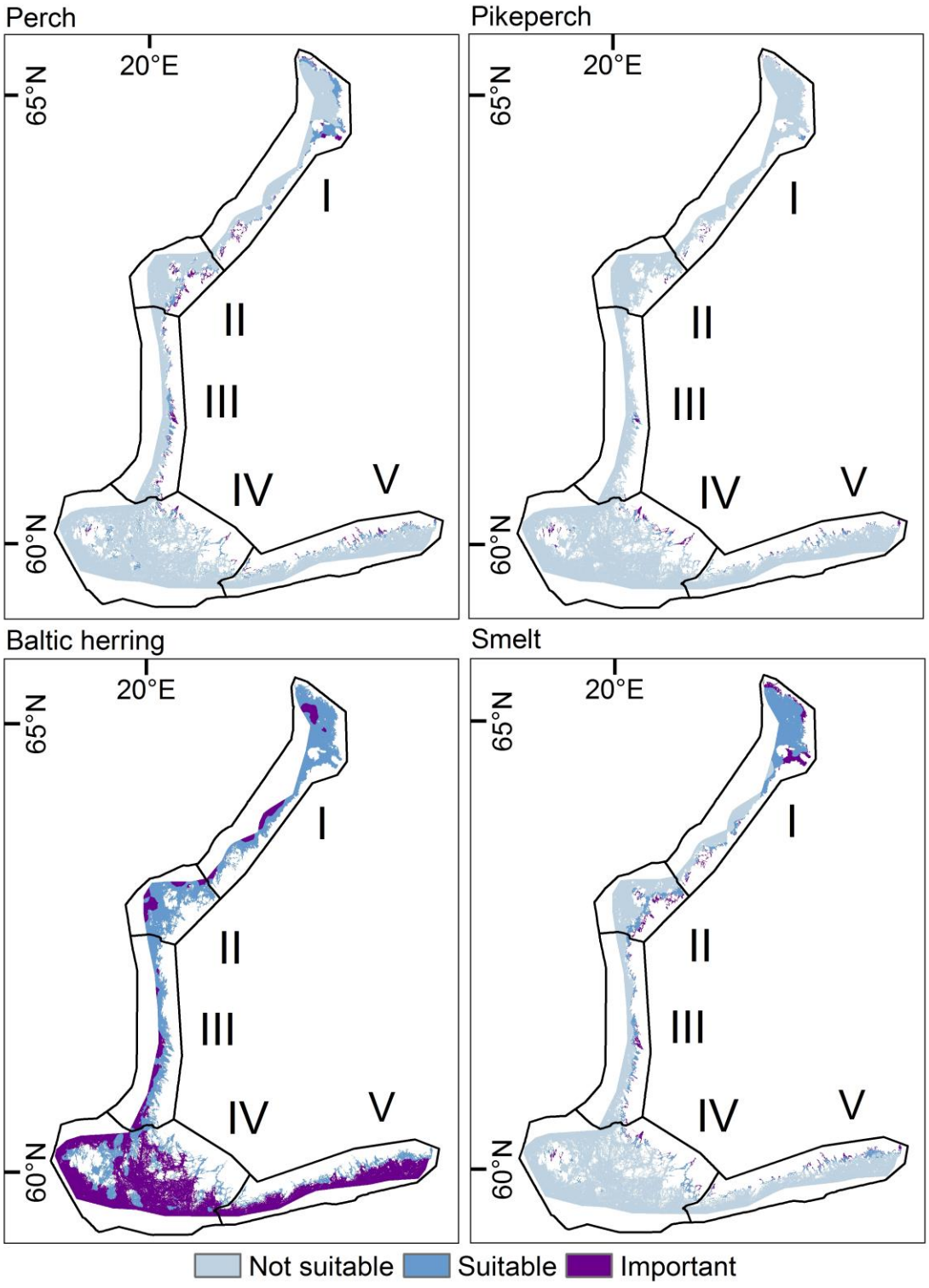

838

839 Figure 3. Predicted larval density maps of perch, pikeperch, Baltic herring, and smelt

840 classified into three classes: not suitable (no larvae expected), suitable (expected area

producing lowest 20% of all larvae), and important (the smallest expected area producing 80% of all larvae).

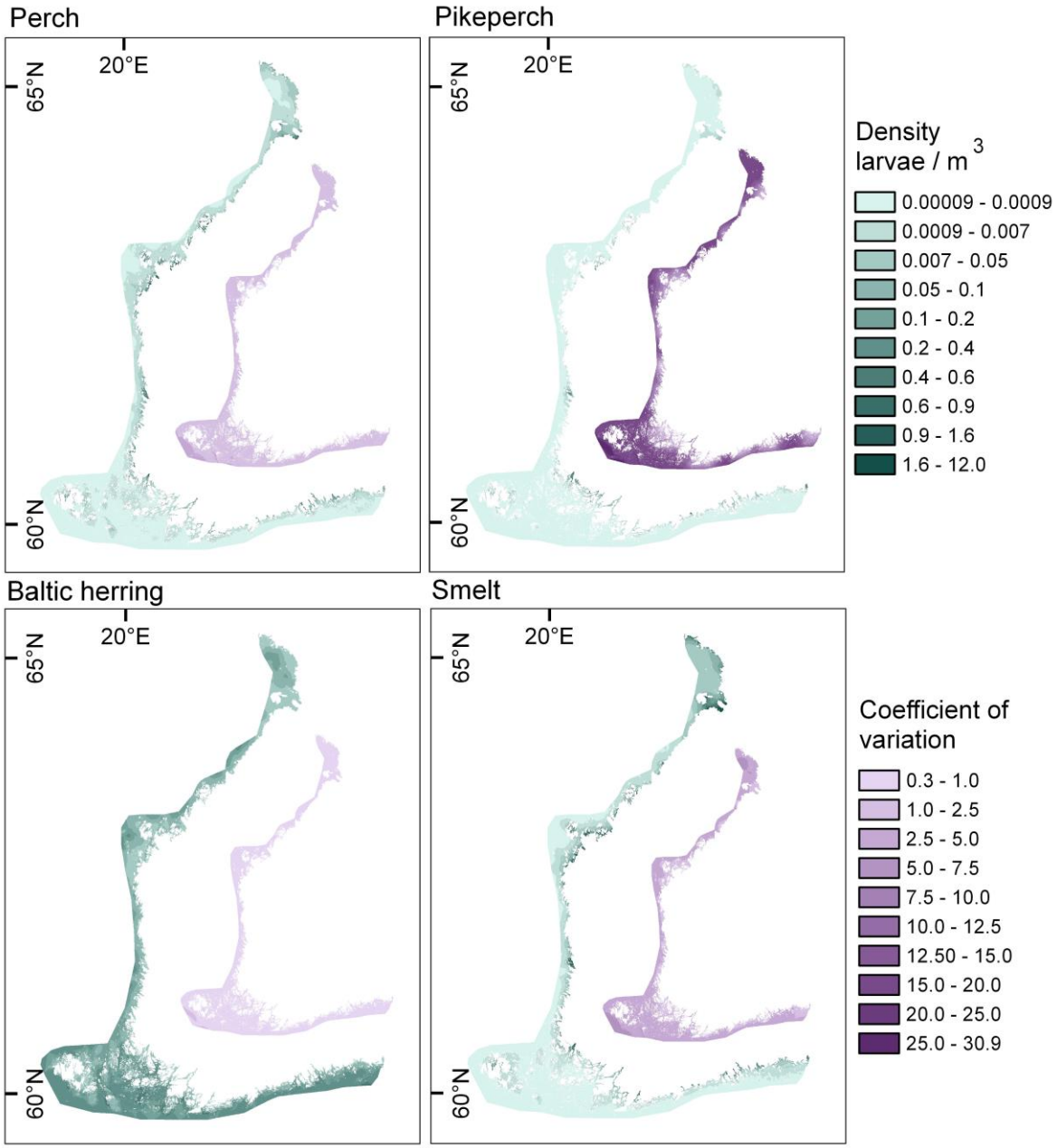

Figure 4. The posterior predictive median (larger maps) and coefficient of variation (smaller maps inside the former) of the larval density of perch, pikeperch, Baltic herring, and smelt.

849 Appendix A1

850

851 Computational details

852

853 We applied Bayes' theorem and calculated the posterior distribution of the
854 covariance function parameters and the latent variables (latent function values corresponding
855 to the observation locations) using the Matlab toolbox GPstuff (Vanhatalo et al. 2013). First,
856 we used the expectation propagation (EP) algorithm to search for the (approximate)
857 maximum a posterior estimate of the covariance function parameters and a Gaussian
858 approximation for the latent variables (see Rasmussen and Williams 2006 and Vanhatalo et
859 al. 2010 for details). EP is a fast approximate algorithm, and its accuracy has been shown to
860 be good in the models we were interested in here (Vanhatalo et al. 2010). Hence, it provides
861 an efficient tool for early "model exploration". After this, we conducted a Markov chain
862 Monte Carlo (MCMC) simulation for the full posterior of covariance function parameters and
863 latent variables by alternating the sampling from conditional distribution of latent variables
864 given covariance function parameters, and vice versa. We used elliptical slice sampling
865 (Murray et al. 2010) for the latent variables and slice sampling (Neal 2003) for the parameters
866 of covariance functions. We sampled 20 000 samples, from which the first 1000 were
867 removed as burn-in. The convergence was checked by the potential scale reduction factor
868 (Gelman et al. 2013). After, this, we thinned the chain to obtain approximately 200
869 independent samples with which the final results were calculated.

870 The interest in this study was in the average larval abundance across the study
871 area. Since the spatio-temporal random effects describe annual changes in larval abundance,
872 we predicted the larval density in grid cells using only the temporally constant terms; that is,

873 we predicted $\tilde{f}(s, x_s) = \alpha + \sum_{d=1}^{D} g_d(x_{s,d}) + h(x_s) + \rho(s)$ in each grid cell and used this to
874 represent the average log larval density between 2007 and 2014. This corresponds to
875 effectively filtering out the temporal changes in the density and can be calculated
876 straightforwardly as presented by Rasmussen and Williams (2006) and Vanhatalo (2010).
877 We calculated the total larval density in an area, A, by a sum of densities in grid
878 cells in that area; that is, $I_{\text{tot}} = \sum_{s_i \in A} e^{\tilde{f}\left(s_i, x_{s_i}\right)}$, where s_i is the coordinate of cell i. Sampling
879 from the posterior distribution of I_{tot} would require first sampling from the joint posterior of
880 f in all grid cells, during which we would need to form the (posterior) covariance matrix of
881 $\tilde{f}$. Since we had over 12 million grid cells in the whole study area, this is infeasible.
882 However, we can calculate the posterior mean and variance of the total density exactly; the
883 former is the sum of expectations over grid cells, $E[I_{\text{tot}}] = \sum_{s_i \in A} E\left[e^{\tilde{f}\left(s_i, x_{s_i}\right)}\right]$, and the latter
884 is the sum of all elements in the covariance matrix $Var[I_{\text{tot}}] =$
885 $\sum_{s_i, s_j \in A} Cov\left[e^{\tilde{f}\left(s_i, x_{s_i}\right)}, e^{\tilde{f}\left(s_j, x_{s_j}\right)}\right]$. Both summaries can be calculated sequentially or the
886 computation can be parallelized and does not involve forming the full covariance matrix.
887 After solving the mean and variance, we approximated the posterior distribution for the total
888 density by a log-Gaussian distribution (Kelsall and Wakefield 2002). In order to speed up the
889 calculations, we used the EP approximation for the posterior when calculating the posterior
890 for the total density. The error from using EP here is negligible, since it provided a good
891 match with the MCMC approximation for the posterior distributions of the latent variables.
892 In order to study the effect of covariates on the larval density, we visualized the
893 expected, zero-centered change in the log density along each covariate. That is, we calculated
894 the posterior of $\tilde{f}(s, t, x_s)\big|_k = f(s, t, x_s)|_k - \bar{f}(s, t, x_s)\big|_k$ along covariate k where
895 $f(s, t, x_s)|_k$ is a function of the kth covariate only when all other covariates are fixed at their

values at location s and $\bar{f}(s,t,x_s)\big|_k = \frac{1}{u_k - l_k}\int_{l_k}^{u_k} f(s,t,x_s)dx_{s,k}$ is the mean of the function over interval $[u_k, l_k]$ along covariate k at that location. We approximated the mean of the function by the arithmetic mean over $M = 20$ equally spaced values along covariate k. Moreover, we calculated the expected response for 50 random locations in order to visualize the effect of the interaction term.

Comparison of models with and without spatial and spatio-temporal random effects

In order to assess the importance of the spatial and spatio-temporal random effects from the posterior predictive point of view we compared our model with models that were otherwise similar but did not include the random effects. We assessed the model performance by using the approximate leave-one-out cross-validation (Vehtari et al. 2014) with log predictive density diagnostics (Vehtari and Ojanen 2012)

$$\sum_{i=1}^{n} \ln p(y_i|x_i, s_i, y_{\setminus i}, x_{\setminus i}, s_{\setminus i}),$$

where $y_{\setminus i}$, $s_{\setminus i}$ and $x_{\setminus i}$ collect all observations, locations and covariates except those related to the ith data point and $p(y_i|x_i, s_i, y_{\setminus i}, x_{\setminus i}, s_{\setminus i})$ denotes the posterior predictive density of the ith observation. A larger log predictive density indicated a better model. The log predictive density statistics are summarized in Table A1.

References

Gelman, A., Carlin, J., Stern, H., Dunson, D., Vehtari, A., and Rubin. D. 2013. Bayesian Data Analysis, Third Edition. Chapman & Hall / CRC Texts in Statistical Science, Miami, USA.

Kelsall, J., and Wakefield, J. 2002. Modeling spatial variation in disease risk: A geostatistical approach. J. Amer. Statist. Assoc. **97**: 692-701.

Murray, I., Adams, R.P., and MacKay, D.J.C. 2010. Elliptical slice sampling. J. Mach. Learn. Res.: Workshop and conference proceedings **9**:541-548.

Neal, R.M. 2003. Slice sampling. Ann. Stat. **31**: 705-767.

Rasmussen, C.E., and Williams, C.K.I. 2006. Gaussian Processes for Machine Learning. The MIT Press, Massachusetts, USA.

Vanhatalo, J. 2010. Speeding Up the Inference in Gaussian Process Models. PhD Thesis, Aalto University, School of Science and Technology.

Vanhatalo, J., Pietiläinen, V., and Vehtari, A. 2010. Approximate inference for disease mapping with sparse Gaussian processes. Stat. Med. **9**: 1580-1607.

Vanhatalo, J., Riihimäki, J., Hartikainen, J., Jylänki, P., Tolvanen, V., and Vehtari A. 2013. GPstuff: Bayesian Modeling with Gaussian Processes. J. Mach. Learn. Res. **14**: 1175-1179.

Vehtari, A., and Ojanen, J. 2012. A survey of Bayesian predictive methods for model assessment, selection and comparison. Stat. Surv. **6**: 142-228.

Vehtari, A., Tolvanen, V., Mononen, T., and Winther, O. 2014. Bayesian leave-one-out cross-validation approximations for Gaussian latent variable models. arXiv:1412.7461v1

940 Table A1. The leave-one-out cross-validation log predictive densities (LPD) and the posterior
941 mode of the overdispersion parameter ($\hat{r}$) of the used models and otherwise similar models
942 from which the spatial and spatio-temporal random effects have been omitted (the higher
943 values are better).
944

	Perch	Pikeperch	Baltic herring	Smelt
	LPD ($\hat{r}$)	LPD ($\hat{r}$)	LPD ($\hat{r}$)	LPD ($\hat{r}$)
Full model	-981.91 (1.18)	-504.15 (14.24)	-1296.17 (1.76)	-1130.33 (2.44)
Full model $-\phi(s,t)$	-981.87 (1.18)	-507.80 (13.84)	-1296.08 (1.77)	-1132.70 (2.14)
Full model $-\rho(s)$	-1013.69 (0.84)	-504.50 (9.65)	-1319.54 (1.18)	-1136.20 (1.78)
Full model $-\rho(s)-\phi(s,t)$	-1058.89 (0.50)	-574.29 (0.82)	-1367.01 (1.17)	-1178.05 (0.94)

945

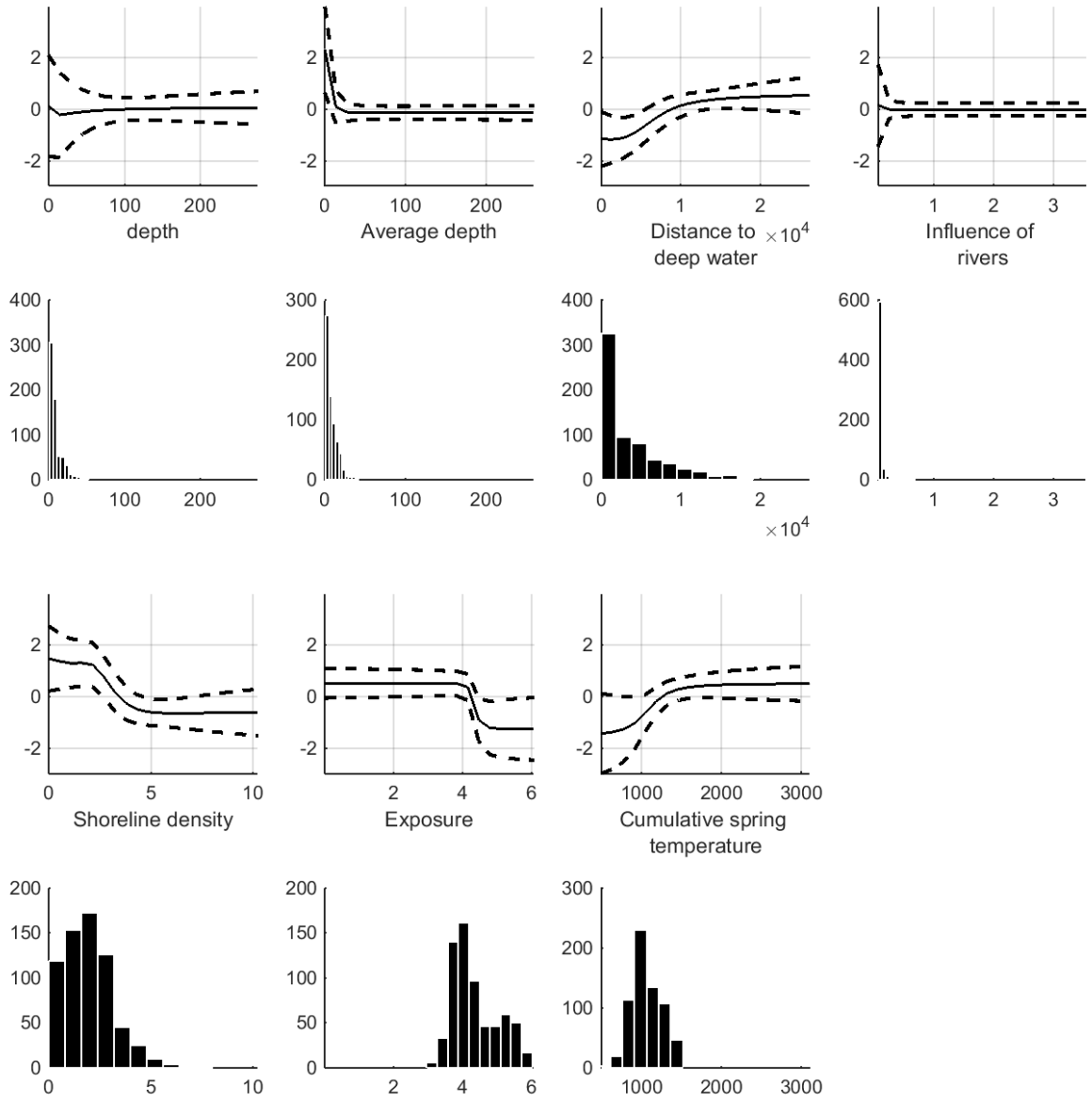

946

947 Figure A1. The response of log-transformed pikeperch larval density along the environmental
948 covariates within the prediction range of the covariates. The solid and dashed black lines
949 describe, respectively, the average response and the 95% credible interval. The histograms
950 show the distribution of covariate values in the data. Notice that when extrapolating the
951 prediction stays at the level where the predictive function was at the end of the data range.
952 This behavior is typical for neural network covariance function. With radial covariance
953 functions, such as the squared exponential, the predictive function would approach prior
954 mean (zero) when extrapolating.